Sub-kHz linewidth Extended-DBR lasers heterogeneously integrated on silicon

Duanni Huang[1*], Minh A. Tran[1], Joel Guo[1], Jon Peters[1], Tin Komljenovic[1], Aditya Malik[1], Paul A. Morton[2], John E. Bowers[1]

1. *Department of Electrical and Computer Engineering, University of California Santa Barbara, CA 93106*
2. *Morton Photonics, West Friendship, MD 21794.*

*duanni@ucsb.edu

Abstract: We demonstrate single-mode E-DBR lasers with 1kHz linewidth and >37mW output power, and ring-assisted E-DBR lasers with 500Hz linewidth, by heterogeneously integrating III-V gain material with a 15mm long ultra-low loss silicon waveguide-based Bragg reflector.

OCIS codes: (140.5960) Semiconductor lasers; (140.3570) Bragg reflectors (140.4780) Optical resonators

1. Introduction

Heterogeneous integration of lasers on silicon through wafer bonding III-V materials onto silicon waveguides has been intensely studied over the past decade and is now mature enough for commercialization, with products for datacom market being shipped in volume. It has been demonstrated that these heterogeneously integrated lasers can outperform even native substrate III-V lasers in some respects such as linewidth, due to lower waveguide loss in silicon. Narrow linewidth lasers are of tremendous importance for applications such as LiDAR and other sensing systems, as well as coherent communications. External cavity lasers using silicon ring reflectors have been shown to achieve kHz-level linewidth and wide tunability, but are complex to operate, as multiple tuning elements must be spectrally aligned, often requiring look-up tables. Distributed Bragg reflector (DBR) lasers are simpler to operate if single-frequency operation is achieved and the linewidth can also benefit from low loss silicon waveguides.

There have been many previous demonstrations of DBR lasers on silicon, with reported linewidths in the MHz range [1]. It has long been known that increasing the cavity length of such a laser will decrease its linewidth [2], although it can lead to poor single-mode behavior and mode hopping using a standard grating design. Hybrid lasers incorporating a high-performance gain chip with an external fiber Bragg grating (FBG) have been developed by Morton Photonics, showing linewidth as low as 15Hz [3]. This is accomplished using a custom, exquisitely fabricated long FBG that provides most of the cavity length, enabling stable, single-mode operation. An extended Bragg grating monolithically integrated with a III-V gain element was not previously realized due to limitations in waveguide loss and grating lithography. We have previously demonstrated ultra-low loss (ULL) silicon waveguides with <0.2dB/cm loss [4], resonators with loaded Q > 2 million, and long Si-based Bragg gratings with a bandwidth less than 50pm that can be seamlessly integrated with our existing heterogeneous silicon/III-V platform [5]. These ULL silicon waveguides consist of a very shallow 56nm etch depth, designed to minimize scattering losses and increase modal volume, which also mitigates nonlinear losses in silicon. Here, we demonstrate the first heterogeneous silicon lasers utilizing these ULL waveguides and extended Bragg reflectors. We achieve record low Lorentzian linewidths of 1kHz for the Extended-DBR (E-DBR) lasers, and 500Hz for a ring assisted version of the E-DBR (RAE-DBR) laser.

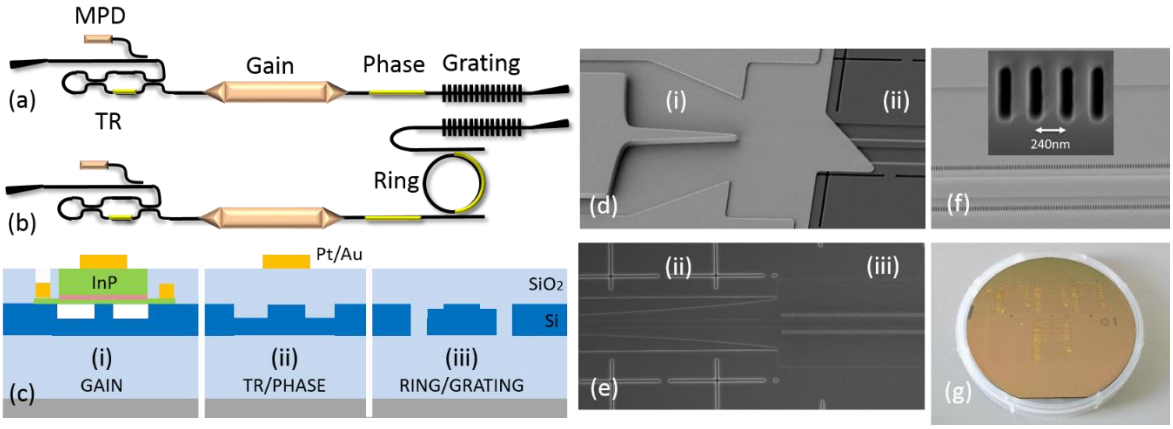

Figure 1: Schematics of the (a) E-DBR and (b) RAE-DBR lasers. (c) Waveguide cross-sections of the different components of the lasers showing bonded III-V material and metal heaters on top of the waveguides. SEM images of the (d) gain to phase control section, (e) phase control to Bragg grating section, and (f) image of the "hole gratings" on each side of the waveguide. The final processed wafer is shown in (g).

2. Design and Fabrication

Schematics of the E-DBR and RAE-DBR lasers are shown in Figs. 1(a) and (b). The E-DBR laser consists of a 2.5mm long gain section, a 0.3mm long phase control section, and a very weak 15mm long Bragg grating. The RAE-DBR has the same gain and phase control section, but a stronger, 10mm long grating, as well as a ring resonator with 0.7mm radius in an add-drop configuration. The waveguide has a different cross-section in each region, which is depicted in Fig. 1(c). The etch depth of the silicon waveguide in the gain and phase region is 231nm out of 500nm total thickness, while it is only 56nm out of 500nm for the waveguide in the Bragg grating and ring resonator. The tapered transitions between each region are designed to be low loss with low reflection; these are depicted in Figs. 1(d) and (e). Further details about these waveguides and transitions can be found in [4].

The Bragg grating is a uniform, first-order grating with a period of 240nm and 50% duty cycle, as shown in Fig. 1(f). These conditions satisfy the Bragg condition near λ = 1563nm for an unperturbed waveguide n_{eff} of 3.2560. Instead of using sidewall or surface etched gratings, we deeply etch holes on either side of the waveguide, allowing us to tailor the coupling coefficient (κ) by varying the distance between the holes and the waveguide, as was previously demonstrated in silicon nitride [6]. This is advantageous in the ultra-low κ regime, as our approach of moving the holes farther away is easier to control compared to conventional approaches for which the sidewall corrugation or surface etch depth becomes very small. A tunable reflector (TR) is formed on the other side of the gain section by combining a tunable Mach-Zehnder interferometer with a loop-mirror. The TR reflectivity can be monitored with the on-chip photodetector (MPD) and adjusted to provide the desired reflectivity. In practice, we tuned this reflector to provide maximum reflectivity, resulting in the lowest threshold current and maximum power out of the Bragg grating side. This should also result in the lowest linewidth for the laser by minimizing the mirror loss.

The fabrication of the lasers can be roughly divided into silicon processing, III-V bonding and processing, and metallization. A 4" SOI wafer with 500nm device layer on 1 micron buried oxide is etched to depths of 56nm for the ULL waveguides, 231nm for the standard rib waveguides, and 500nm for the hole gratings and outgassing channels. DUV lithography is used to pattern the waveguides, while the gratings are defined using e-beam lithography. III-V gain materials containing 3 InAlGaAs quantum wells are directly bonded and subsequently processed to form the laser mesas, before the contacts are finally deposited. Further fabrication details can be found in [7]. An image of the fully processed wafer is shown in Fig. 1(g) prior to sample dicing and facet polishing.

3. Characterization

Lasers are characterized on a temperature-controlled stage at room temperature. The TR is set to provide maximum reflection, and light is coupled out through the grating side into a lensed fiber. The coupling loss is measured to be 6.5dB through calibration with a broad-area photodetector. The LIV for the DBR is shown in Fig. 2(a), showing a threshold current of 50mA and maximum on-chip (fiber-coupled) power of 37mW (8.3mW). Kinks in the laser power correspond to longitudinal mode hopping in the E-DBR due to heating of the gain section causing the longitudinal mode to be detuned from the grating peak. Operating the E-DBR near the mode hops can result in multimode, chaotic, or self-pulsing behavior [8]. We avoid these mode hops by actively tuning the phase section along with the gain, resulting in a smoother LIV, indicative of stable, single mode behavior (Fig. 2(a) blue). The SMSR is nearly 60dB.

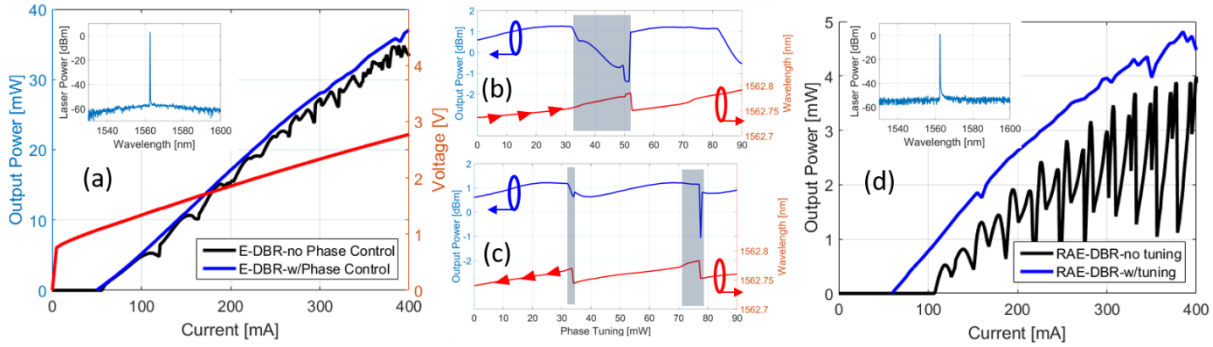

Figure 2: (a) LIV curve and spectra (inset) of the DBR with and without phase adjustment. At a fixed gain of 200mA, the laser encounters different multi-mode regimes, which are shaded, depending on whether the longitudinal modes are (b) redshifted or (c) blueshifted. (d) LIV curve and spectra of the RA-E-DBR with and without ring and phase adjustment.

We study these lasing mode effects in more detail by sweeping the power to the phase section (up and down) for 200mA gain current as shown in Fig. 2(b) and (c). We notice a strong drop in laser output power prior to a mode hop, which is confirmed to be multimode using a high resolution OSA. The laser displays hysteresis effects where these mode hops happen when sweeping the phase power up and down. It also appears to be more stable when decreasing the phase power, which shifts the longitudinal modes to shorter wavelengths. This may be due to the slightly

asymmetric spectral response of the grating, as we later discuss. The LIV of the RAE-DBR is shown in Fig. 2(d) with and without tuning the ring. The ring should be aligned to the grating to minimize losses, after which we observe a threshold current of 60mA and output on-chip power of 4.8mW. The output power of the RAE-DBR is lower than the DBR due to the losses (propagation and coupling) going through the ring twice as well as higher mirror loss due to the stronger grating. These losses may be mitigated by weakening the grating and/or moving the ring to the left-hand side to be included in the loop mirror to allow effectively only one pass through the ring per round trip.

We can measure the exact spectral transmission response of the grating reflector by injecting light from an external tunable laser through the grating and measuring the photocurrent in the gain section. From this measurement, we can extract the bandwidth (25pm) and reflectivity (40%) of the passive Bragg reflector in Fig. 3(a), from which we estimate our κL to be 0.65. The side-lobes of the grating are slightly asymmetric, likely due to nonuniformity along the length of the grating. The measurement procedure can also be used to scan the passive RAE-DBR in Fig. 3(b), which is the product of the Bragg grating and ring transmission. The measurement shows that the ring transmission is suppressed at the Bragg wavelength. While we cannot directly calculate the RAE-DBR reflectivity from this, it provides insight on the ring bandwidth (3pm) and grating reflectivity (>85%). This supports our findings that the linewidth for the RAE-DBR is lower due to the larger effective cavity length, although it has lower output power.

The frequency noise of the lasers is measured using a Sycatus/Keysight optical noise analyzer. We observe a white-noise limited frequency noise of 350Hz^2/Hz and 170 Hz^2/Hz for the E-DBR and RAE-DBR lasers respectively in Fig. 3(c), corresponding to about 1kHz and 500Hz Lorentzian linewidths after multiplying by π. The relative intensity noise (RIN) measured for the E-DBR are shown in Fig. 3(d) at several drive currents. There are several peaks in the 0-10GHz range, which may be attributed to mode beating between the lasing mode and non-lasing cavity modes. Optimal phase control and grating apodization could suppress these peaks. For 200mA drive current, the RIN is measured to be less than -150dB/Hz apart from the dominant peak at 7GHz.

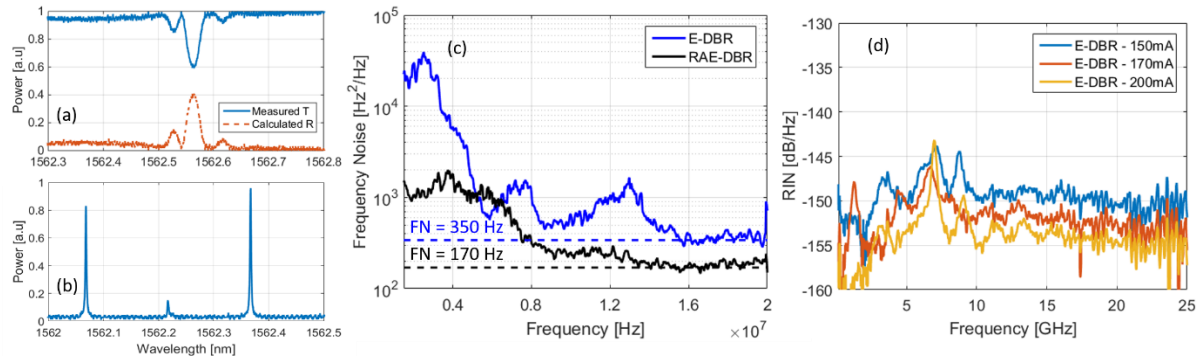

Figure 3: Passive spectral characterization of the (a) E-DBR and (b) RAE-DBR showing 25pm and 3pm full-width half max respectively. (b) Frequency noise measurement for the lasers and (c) RIN noise measurements for the E-DBR.

4. Conclusions

We demonstrate heterogeneously integrated E-DBR lasers on silicon with 1kHz linewidth and over 37mW of output power. Adding a high-Q ring into the cavity further reduces the linewidth to 500Hz, however, with an output power of 4.8mW. The narrow linewidth is achieved by using ultra low loss silicon waveguides and extremely low κ gratings to form a 15mm long DBR. Future work includes grating apodization to increase SMSR and reduce multimode effects, as well as improved design of the ring in the RAE-DBR to minimize losses.

Acknowledgements

The authors acknowledge funding through Morton Photonics DARPA STTR program #W911NF-16-C-0072, and to Sycatus/Keysight for the loan of frequency noise measurement equipment.

References

[1] S. Keyvaninia, et al. "Demonstration of a heterogeneously integrated III-V/SOI single wavelength tunable laser." Opt. Express **21**(3), 3784-3792 (2013).

[2] C. Henry, "Theory of the linewidth of semiconductor lasers", IEEE J. Quantum Electron. **18**(2), 259-264 (1982).

[3] P. A. Morton and M. Morton "High-Power, Ultra-Low Noise Hybrid Lasers for Microwave Photonics and Optical Sensing", J. of Light. Technol. (2018).

[4] M. A. Tran et al., "Ultra-Low-Loss Silicon Waveguides for Heterogeneously Integrated Silicon/III-V Photonics", Appl. Sci. **8**, 1139 (2018).

[5] T. Komljenovic, et al. "Photonic Integrated Circuits Using Heterogeneous Integration on Silicon." Proc. of the IEEE **99**, 1-12(2018).

[6] D. T. Spencer, et al., "Low kappa, narrow bandwidth Si3N4 Bragg gratings", Opt. Express **23**(23), 30329-30336 (2015).

[7] M. L. Davenport, "Heterogeneous Silicon III-V Mode Locked Lasers", dissertation (2017).

[8] X. Pan, et al., "A Theoretical Model of Multielectrode DBR Lasers", IEEE J. Quantum Electron. **24**(12), 2423-2432 (1988).